COMMUNICATION

Versatile strained alkyne modified water-soluble AuNPs for *interfacial* strain promoted azide–alkyne cycloaddition (I-SPAAC)†

Pierangelo Gobbo,[a] Zack Mossman,[a] Ali Nazemi,[a] Aurelia Niaux,[a] Mark C. Biesinger,[b] Elizabeth R. Gillies[ac] and Mark S. Workentin*[a]

Versatile water- and organic solvent-soluble AuNPs that incorporate an interfacial strained alkyne capable of efficient pour and mix strain promoted interfacial cycloadditions with azide partners have been synthesized and carefully characterized for the first time. The use of XPS to quantitate the loading of the strained alkyne on the AuNPs is noteworthy. The reactivity towards the *interfacial* strain promoted azide–alkyne cycloaddition reaction was demonstrated by using azide-decorated polymersomes as bioorthogonal reaction partners.

The strain promoted alkyne–azide cycloaddition (SPAAC) is a bioorthogonal reaction designed as a tool for *in vivo* imaging and tracking of biomolecules. The power of this reaction relies on its rapid kinetics, chemoselectivity and biocompatibility. Therefore, it represents an important technological step that not only allows the spatial resolution of living organisms, but also furnishes unique temporal aspects of bioprocesses that happen *in vivo*.[1–8] Recent success in the application of the SPAAC reaction has been shown by C. R. Bertozzi and co-workers to follow *in vivo* the glycan evolution during the zebrafish development.[9,10] These characteristics not only make this reaction highly useful in biochemistry, but also provide invaluable opportunities in designing new materials. Surprisingly, given its broad application in biological applications, the use of the SPAAC reaction has been limited in the latter context so far. The SPAAC reaction has been used for the synthesis of dendrons and dendrimers.[11–13] Johnson and co-workers used the reaction to synthesize photodegradable star polymers.[14] Popik and co-workers prepared dibenzocyclooctyne (DBCO)-modified glass, silicon and quartz surfaces and showed their potential applications as platforms for the generation of multicomponent surfaces.[15,16] Bernardin and co-workers synthesized monosaccharide-functionalized quantum dots for *in vivo* metabolic imaging through the reaction between cyclooctyne-modified quantum dots and azide modified monosaccharides.[17] Recently we employed the SPAAC to create a carbon nanotube (CNT)–AuNP hybrid material by the interfacial reaction between a DBCO-modified CNT and an azide-modified AuNP.[18]

For the first time, we describe here a method for the synthesis of AuNPs that incorporate an interfacial strained alkyne moiety that can be used as a reactive template and undergo an *interfacial* SPAAC reaction (I-SPAAC) with azide modified reagents. A particular strength of this method is that it allows for a careful quantification of the amount of interfacial strained alkynes. This information is of particular relevance for potential application of these AuNPs in drug delivery and bioconjugation. The amount of interfacial strained alkynes was estimated through two independent methods: a combination of TGA and ^{1}H NMR data,[19] and through high-resolution XPS analysis. This novel bioorthogonal nanomaterial represents a desirable template for diverse applications thanks to its biocompatibility (unlike quantum dots) and the size dependent properties of AuNPs combined with the reactivity properties of the SPAAC. In particular the rapid chemoselective reaction of these DBCO–nanoparticles is the main factor that distinguishes this novel nanomaterial from other clickable nanoparticles (*i.e.* maleimide-functionalized nanoparticles) commonly used for bioconjugation and drug delivery.[20–23] Another important characteristic is that it displays both organic solvent solubility and water-solubility, despite the strong organic character of the interfacial DBCO moieties. The water-soluble AuNP based on tri- and tetra-ethylene glycol ligands that are used as the scaffold for our synthesis serves as a phase-transfer agent for overcoming one of the major drawbacks of the SPAAC reaction, which is the poor solubility of strained alkynes in water media.[1,24] For these reasons the DBCO–AuNPs represent an extremely versatile framework that can be functionalized with potentially any azide modified molecular systems in an easy and straightforward way. Herein, as proof of concept, we used azide-functionalized

[a] The University of Western Ontario and the Centre for Materials and Biomaterials Research, Richmond Street, London, Ontario, Canada. E-mail: mworkent@uwo.ca; Tel: +1 519-661-2111 ext. 86319

[b] Surface Science Western, The University of Western Ontario, 999 Collip Circle, London, Ontario, N6G 0J3, Canada

[c] Department of Chemical and Biochemical Engineering, The University of Western Ontario, London, Ontario, Canada

polymersomes as their reacting partners to show the potential of the DBCO–AuNPs in constructing covalent biohybrid materials, and furnishing the first example of an I-SPAAC reaction on the new strained alkyne-functionalized AuNPs. The resulting hybrid materials were prepared simply through a pour and mix chemistry in aqueous media, and the resulting vesicles were found to be functionalized with ∼3 nm AuNPs.

Scheme 1 shows our approach to the synthesis of DBCO–AuNPs. This approach must take into account the reactivity of the strained alkynes towards nucleophiles.[6,25–27] In fact, a thiol-functionalized strained alkyne ligand for rapid incorporation into the AuNPs *via* place-exchange reaction is unsuitable because it would rapidly self-react. For this reason we exploited an interfacial amide coupling reaction between a carboxy-terminated AuNP ligand and a DBCO-amine, which could be run in organic solvents thanks to the amphiphilic properties of the prepared HOOC–AuNPs given by the ethylene glycol-based ligands. This reaction was selected because of its high yield, the product is resistant to hydrolysis allowing for applications in water media, and the formation of the new interfacial amide bond can be easily followed by IR spectroscopy and XPS, furnishing important quantitative data (*vide infra*). The first synthesis step was therefore the synthesis of methyl-terminated triethylene glycol monolayer-protected AuNPs (Me–EG$_3$–AuNPs) following our previously established procedure.[28] Briefly, HAuCl$_4$·3H$_2$O was mixed for 1 hour with 3 molar equivalents of Me–EG$_3$–SH using a methanol–acetic acid mixture as the solvent. To the resulting bright yellow solution a water solution of NaBH$_4$ was added resulting in a dark brown solution typical of the formation of 2.8 ± 0.6 nm AuNPs, as determined from TEM images. For further details refer to the ESI.† Subsequently, the Me–EG$_3$–AuNP underwent the place-exchange reaction to introduce ω-carboxy tetra-ethylene glycol thiols (HOOC–EG$_4$–SH). The place-exchange reaction was carried out in CH$_2$Cl$_2$ for 30 min at room temperature. The free thiols (Me–EG$_3$–SH and HOOC–EG$_4$–SH) were removed by washing the nanoparticle film formed inside the reaction vessel after removing CH$_2$Cl$_2$, with hexanes and isopropanol, in which the carboxy-functionalized AuNPs (HOOC–EG$_4$–AuNPs) are not soluble. These carboxy-terminated AuNPs were found to be water-soluble and soluble in DMF and DMSO. HOOC–EG$_4$–AuNPs were characterized by ^{1}H NMR and IR spectroscopy, TEM, TGA and XPS. The ^{1}H NMR spectrum recorded in D$_2$O (Fig. 1) shows the typical broad peaks of a AuNP sample, confirming the success of our washing

procedure. The success of the place-exchange reaction was then confirmed by the appearance of a peak at 4.11 ppm corresponding to the two protons belonging to the carbon alpha of the carboxylic acid group in the carboxy-terminated ligands. Through the integration of the peak at 4.11 ppm and the integration of the peak at 3.32 ppm, which belongs to the three protons of the methyl group of the Me–EG$_3$–S$^-$ ligands, it was possible to determine that 26 ± 5% of the ligands composing the monolayer that protects the gold core was composed of HOOC–EG$_4$–S$^-$, while 74 ± 5% was composed of Me–EG$_3$–S$^-$. This composition allows the amphiphilic property of the AuNPs to be maintained and therefore permits the subsequent coupling reaction in the organic solvent where it is more efficient. A higher content of the HOOC–EG$_4$–S$^-$ ligand would result in AuNPs that are exclusively water-soluble. The IR spectrum of the purified HOOC–EG$_4$–AuNP shows the appearance of the carbonyl stretching signal at 1740 cm^{-1}, confirming the presence of carboxylic moieties on the AuNP (see Fig. S9†). TEM images show that HOOC–EG$_4$–AuNPs maintain the same gold core diameter of 2.8 ± 0.6 nm of the starting material Me–EG$_3$–AuNPs (Fig. S4†). The derivative of the TGA curve (Fig. S5†) shows that the two ligands decompose at two different temperatures. The Me–EG$_3$–S$^-$ decomposes at 265 °C, while the HOOC–EG$_4$–S$^-$ decomposes at 315 °C. The assignment of the two peaks to the corresponding ligands was carried out by analyzing three different HOOC–EG$_4$–AuNP samples containing an increasing amount of carboxy-functionalized ligands, and comparing their TGA results with the corresponding ^{1}H NMR spectra. It was then possible to calculate that the HOOC–EG$_4$–AuNPs contain the carboxylic group in a concentration of
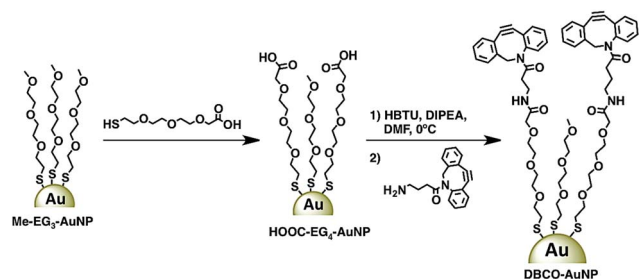
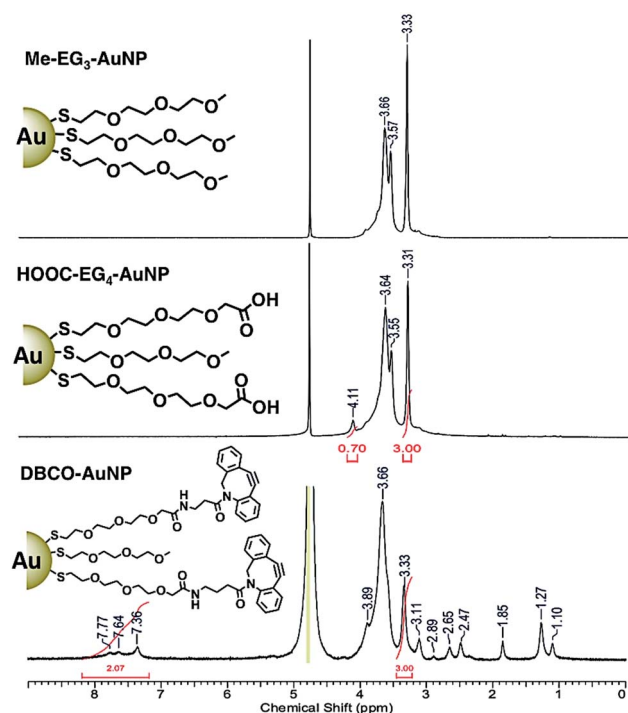Scheme 1 Outline of the synthesis strategy employed to synthesize the DBCO–AuNP.

Fig. 1 ^{1}H NMR spectra of the AuNPs after each synthesis step recorded in D$_2$O. Spectra calibrated against residual H$_2$O.

$0.46~\mu mol~mg^{-1}$. From the combination of the ^{1}H NMR, TGA and TEM data, and assuming that the AuNPs are spherical and that their size is monodispersed (2.8 nm), it was possible to calculate an approximate molecular formula for the HOOC–AuNPs of $Au_{500}(Me-EG_3-S)_{280}(HOOC-EG_4-S)_{100}$.[19]

XPS analysis further confirmed the successful synthesis of HOOC–EG_4–AuNPs and the ratio between the two different ligands that surround the gold core. The Au $4f_{7/2}$ core line appears at 84.3 eV, which is shifted to a binding energy higher than that of the bulk gold (83.95 eV) due to particle size effects.[29] The S 2p core line shows the presence of two major components, S $2p_{3/2}$ at 162.8 eV and S $2p_{1/2}$ at 164.0 eV, in a 2 : 1 spin–orbit splitting ratio for the Au–S bonds, and just 11% of unbound thiol characterized by two components in a 2 : 1 ratio at 163.8 eV $(2p_{3/2})$ and 165.0 eV $(2p_{1/2})$, respectively.[30] Finally, the high-resolution scan of the C 1s peak and the O 1s peak (see Fig. 2) confirmed the presence of carboxylic functionalities on the gold cores. The O 1s core line shows the appearance of a shoulder at 533.7 eV that corresponds to $-(C=O)-OH$, while the C 1s core line shows the appearance of an isolated component at 289.3 eV typical of the carboxylic functional group. From the molecular structure of the two ligands that surround the gold core and from the relative percentages of the C 1s component at 289.3 eV and that at 286.3 eV related to C–O of the ethylene glycol units of both the ligands, it was possible to estimate the composition of the organic layer protecting the gold core with good precision. Through this independent method we could confirm that $26 \pm 2\%$ of the ligands were $HOOC-EG_4-S^-$. Details of the calculation are reported in the ESI.†

The DBCO-amine was then reacted with the HOOC–AuNPs using HBTU as a coupling agent. In a typical synthesis, HOOC–AuNPs (65 mg, 30 μmol of –COOH) and N,N-diisopropylethylamine (16 μl, 90 μmol) were dissolved in 10 ml of dry DMF in a round bottom flask. The solution was then cooled down to 0 °C and purged with argon gas. To this solution was added HBTU (23 mg, 60 μmol) dissolved in 5 ml of dry DMF. The reaction

mixture was stirred at 0 °C for 15 min and then a solution of DBCO-amine (17 mg, 60 μmol) in 3 ml of dry DMF was added. The reaction was allowed to progress overnight in an inert atmosphere. The DBCO–AuNP was purified through dialysis using a 6–8 kDa MWCO membrane against DMF in order to remove the organic byproducts, followed by dialysis against water in order to remove DMF. The DBCO–AuNP was characterized by ^{1}H NMR and IR spectroscopy, TEM and XPS. ^{1}H NMR spectroscopy recorded in D_2O (see Fig. 1) showed the disappearance of the peak at 4.11 ppm, the concomitant appearance of aromatic protons between 7 and 8 ppm related to the aryl rings of DBCO and new peaks between 1 and 3 ppm. Through the integration of the aromatic protons and that of the reference peak at 3.32 ppm, corresponding to the $Me-EG_3-S^-$ ligands, it was possible to determine that $21 \pm 5\%$ of the ligands (0.10 μmol per mg of DBCO) were successfully modified with DBCO. XPS confirmed this result and furnished proof of interfacial reactivity, showing the appearance of the peak related to the amide nitrogens introduced with the DBCO-amine at 400.3 eV, a marked decrease of the carboxylic group components (O 1s at 533.7 eV and C 1s at 289.3 eV), and the concomitant appearance of the components of $-(C=O)-NH-$ at 531.7 eV and that of $-(C=O)-NH-$ at 288.3 eV (see Fig. 2 and S8†). Through the abundance of the nitrogen peak with respect to the initial abundance of $-(C=O)-OH$ it was possible to calculate an 80% yield for the interfacial coupling reaction. This extent of interfacial reaction was confirmed by using the ratio between the percentage of the C 1s peaks from the residual carboxylic acid carbonyl carbon and that of the amide C=O at 288.3 eV and 289.3 eV, respectively. IR spectroscopy (see Fig. S9†) further confirmed the success of the interfacial coupling reaction showing the appearance of the typical amide stretching signal at $1658~cm^{-1}$ and the N–H stretching signal at $3420~cm^{-1}$, and a marked decrease of the carbonyl signal at $1730~cm^{-1}$. As expected, TEM images did not show any significant change in the size distribution of the nanoparticles after the interfacial coupling reaction because of the mild reaction conditions. Finally, the ζ-potential of the DBCO–AuNP in PBS of pH 7.0 was found to be −36.4 mV indicating good stability of the nanoparticles in water solution.

As a proof of concept and to highlight the reactivity of DBCO–AuNPs towards the I-SPAAC reaction, the nanoparticles were reacted with azide-decorated polymersomes.[31] These polymersomes were prepared from a PBD–PEO–N_3 block copolymer (see Fig. 3) (for synthesis details please refer to the ESI†) and were extruded 2 times through 1000 nm, 400 nm, 200 nm and 100 nm polycarbonate membranes (see ESI†). In a typical reaction 0.05 mg of DBCO–AuNPs were mixed with 0.5 mg of azide-decorated polymersomes in 1 ml of distilled water for 1 hour. A molar excess of 10 : 1 of azide with respect to the DBCO functional group was employed to ensure complete reactivity of the AuNPs with the polymeric vesicles. The success of the interfacial reaction was then verified through TEM. Fig. 3 and S10† clearly show that the polymersome surfaces have been successfully functionalized with ~3 nm AuNPs, displaying well-defined and easy to image vesicles, thanks to the contrast given by the metallic nanoparticles. A control experiment was then carried
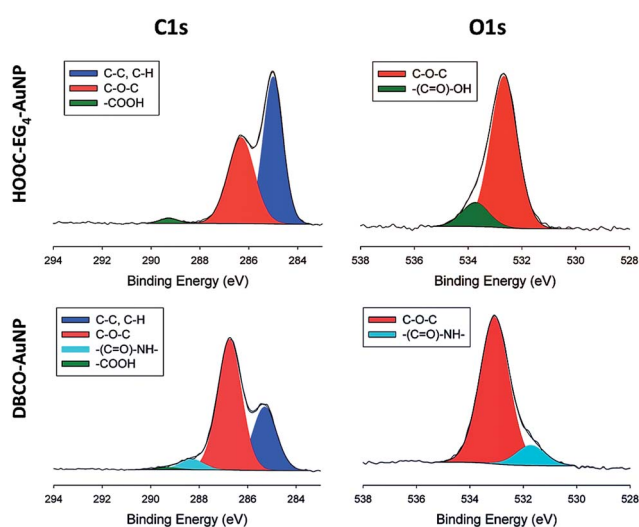

Fig. 2 High-resolution C 1s and O 1s XPS spectra for HOOC–EG_4–AuNPs and DBCO–AuNPs.

1766 | J. Mater. Chem. B, 2014, 2, 1764–1769

This journal is © The Royal Society of Chemistry 2014

out to verify that the presence of the nanoparticles was not due to unspecific interactions. This experiment was carried out under the same conditions as before but instead of using the DBCO–AuNPs, Me–EG$_3$–AuNPs were employed. The TEM images of the control experiment (Fig. 3a and S11†) only show a limited number of AuNPs randomly scattered on the TEM grid and vesicles that are faint and difficult to distinguish because of the lack of specific interactions. The comparison between Fig. 3A and B clearly shows that the AuNP-decorated vesicles can be obtained through the I-SPAAC reaction using the DBCO–AuNPs. The great impact of the DBCO–AuNPs relies on their ease of reaction with azide-functionalized molecular systems through a straightforward pour and mix chemistry under mild reaction conditions. This approach represents an important breakthrough in the AuNP interfacial click-chemistry because of the numerous problems related to the more well known copper catalyzed version of the azide–alkyne cycloaddition (also know as copper catalyzed [3 + 2] Huisgen cycloaddition), normally employed to create bioconjugates and other hybrid materials. In fact, the Cu-catalyzed azide–alkyne cycloaddition at the AuNP interface is known to give very low cycloaddition yields and to cause severe AuNP aggregation/decomposition due to the reaction of Cu(I) salt with the gold surface and to the presence of reducing agents commonly employed to reduce in situ CuSO$_4$.[32] Different attempts have been reported in the literature to try improve the reaction efficiency at the AuNP interface, but they involve very harsh reaction conditions (e.g. very long reaction times[33,34] or massive excess of reagents[34,35]) or the use of particular instrumentation (e.g. microwave[36] or very high pressure[32]) that strongly limits its versatility. To show the improvement that our copper-free approach brings to this scenario, we compared the two different reactions (Cu-free vs. Cu-catalyzed) using small water-soluble azide modified AuNPs (azide-AuNPs). The azide-AuNPs were synthesized following our previously established procedure (see ESI†) and were reacted with two different alkynes (2-propyn-1-amine hydrochloride and 1-ethynylpyrene) using standard procedures reported in the literature.[36] We made different attempts to carry out the copper catalyzed [3 + 2] Huisgen cycloaddition but all the experiments resulted in TEG–AuNP aggregation or, using lower reaction times, in negligible reactivity (see ESI†). When instead the azide–AuNPs were exposed to DBCO-amine, the cycloaddition product was detected by ^{1}H NMR spectroscopy with only 1 hour of reaction time (see ESI†) and with a 60% cycloaddition yield. The use of the I-SPAAC reaction in place of the copper catalyzed [3 + 2] Huisgen cycloaddition not only allows preservation of the stability of the colloidal solution and makes the cycloaddition more efficient, but also allows the reaction to occur under physiological conditions, avoiding the use of the toxic copper catalyst.

For the first time we describe a simple synthesis and characterization of water-soluble AuNPs that incorporate an interfacial strained alkyne functionality, DBCO, able to efficiently
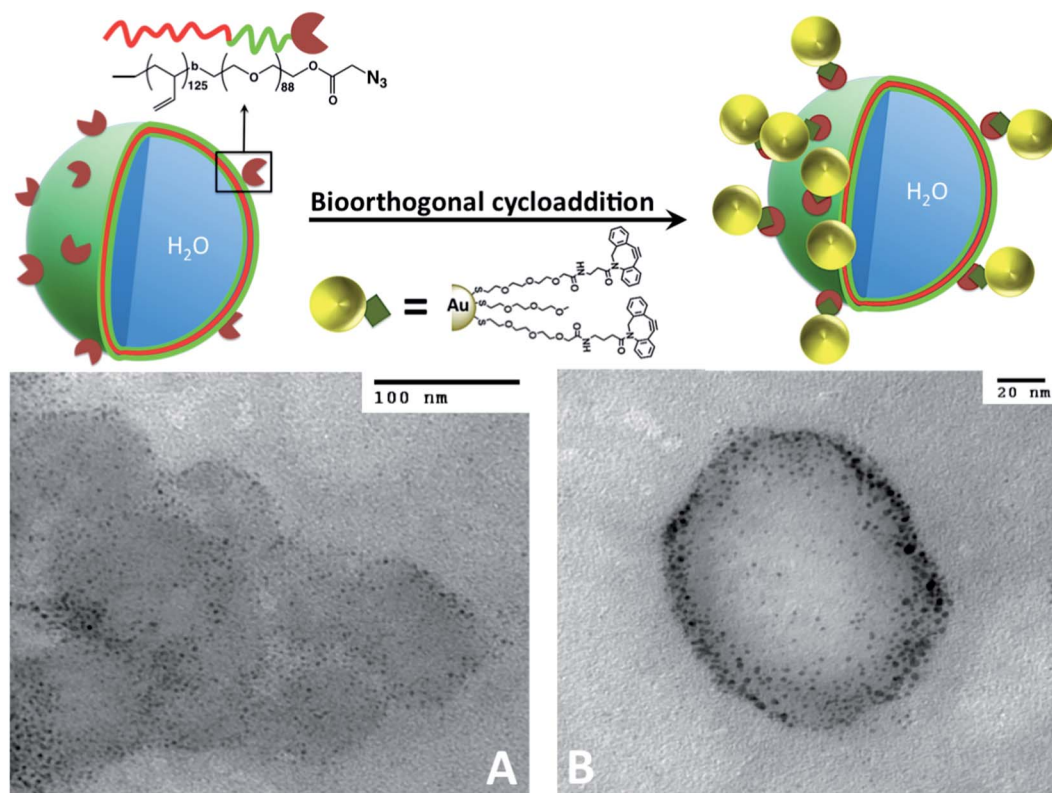

Fig. 3 Top: a cartoon representing the I-SPAAC reaction between DBCO–AuNPs and azide-functionalized polymersomes. (A) TEM image of the control experiment Me–EG$_3$–AuNP + azide-functionalized polymersomes. (B) TEM image of vesicles covered with AuNPs through the I-SPAAC reaction.

This journal is © The Royal Society of Chemistry 2014

J. Mater. Chem. B, 2014, 2, 1764–1769 | 1767

undergo an I-SPAAC reaction in aqueous media with nano-materials despite the exclusively organic solvent solubility of the DBCO moieties. The synthesis method presented takes into account the reactivity of the strained alkyne towards nucleophiles and involves an interfacial amide coupling reaction between carboxy-terminated AuNPs and a DBCO-amine. The same approach can also be used for coupling diverse amine-functionalized strained alkynes with different reaction kinetics toward the dipolar cycloaddition,[1] allowing the synthesis of strained-alkyne-functionalized AuNPs with tunable reactivity towards the I-SPAAC reaction. The DBCO–AuNPs were characterized through ^{1}H NMR spectroscopy, IR spectroscopy, TGA, TEM, and XPS and the amount of DBCO on the corona was estimated with good precision through two independent methods. In particular we demonstrated that XPS is a powerful tool not only for qualitatively monitoring the interfacial reactivity, but also for quantifying with higher precision the newly introduced interfacial moieties. This quantification methodology can be transferrable also to larger particles. The precise quantification of the interfacial strained alkyne moieties is of great importance for the application of these nanoparticles in bioconjugation and drug delivery. To showcase the power of the interfacial reactivity of the DBCO–AuNPs, the nanoparticles were used to react with azide-decorated polymersomes. Polymersomes were selected because a visual proof of the I-SPAAC reaction can be easily obtained through electron microscopy, because they mimic the structures of cell membranes, and are emerging as highly promising, potentially multifunctional vehicles that have been used in a wide range of biomedical applications such as drug delivery and imaging.[37–40] The covalent attachment of inorganic nanoparticles into these structures is of significant interest in order to tune the chemical and physical properties of the materials and to obtain new properties that result from the synergistic combination of the organic and inorganic components.[41–43] Finally, by comparing the I-SPAAC reaction with its Cu-catalyzed version, we showed that our strategy leads to a high yield for the interfacial reaction and preserves the stability of the AuNP. In addition it provides a copper-free environment necessary for potential applications of these DBCO–AuNPs *in vivo*.

Thanks to the intrinsic biocompatibility of these new AuNPs coupled with the chemoselectivity and the fast reaction kinetics towards the azide group conferred by the interfacial strained alkyne, the DBCO–AuNPs represent not only promising versatile scaffolds for the facile and efficient modification of material interfaces, but also represent a powerful tool exploitable in biochemistry, biology and nanomedicine. Indeed the *in vivo* labeling of azide modified biomolecules and tissues can be easily achieved through the methodology herein described, seeing the relative ease of introduction of azide functionalities in the biosystems compared to the introduction of strained alkynes. These possibilities are currently being explored.

Acknowledgements

Notes and references

1 M. F. Debets, S. S. Van Berkel, J. Dommerholt, A. J. Dirks, F. P. J. T. Rutjes and F. L. Van Delft, *Acc. Chem. Res.*, 2011, **44**, 805–815.

2 J. C. Jewett and C. R. Bertozzi, *Chem. Soc. Rev.*, 2010, **39**, 1272–1279.

3 M. D. Best, *Biochemistry*, 2009, **48**, 6571–6584.

4 H. L. Evans, R. L. Slade, L. Carroll, G. Smith, Q. D. Nguyen, L. Iddon, N. Kamaly, H. Stockmann, F. J. Leeper, E. O. Aboagye and A. C. Spivey, *Chem. Commun.*, 2012, **48**, 991–993.

5 H. L. Evans, L. Carroll, Q. D. Nguyen, E. O. Aboagye and A. Spivey, *J. Labelled Compd. Radiopharm.*, 2013, **56**, S204.

6 K. E. Beatty, J. D. Fisk, B. P. Smart, Y. Y. Lu, J. Szychowski, M. J. Hangauer, J. M. Baskin, C. R. Bertozzi and D. A. Tirrell, *ChemBioChem*, 2010, **11**, 2092–2095.

7 J. Dommerholt, S. Schmidt, R. Temming, L. J. A. Hendriks, F. P. J. T. Rutjes, J. C. M. van Hest, D. J. Lefeber, P. Friedl and F. L. van Delft, *Angew. Chem., Int. Ed.*, 2010, **49**, 9422–9425.

8 X. H. Ning, J. Guo, M. A. Wolfert and G. J. Boons, *Angew. Chem., Int. Ed.*, 2008, **47**, 2253–2255.

9 K. W. Dehnert, J. M. Baskin, S. T. Laughlin, B. J. Beahm, N. N. Naidu, S. L. Amacher and C. R. Bertozzi, *ChemBioChem*, 2012, **13**, 353–357.

10 S. T. Laughlin, J. M. Baskin, S. L. Amacher and C. R. Bertozzi, *Science*, 2008, **320**, 664–667.

11 B. C. Sanders, F. Friscourt, P. A. Ledin, N. E. Mbua, S. Arumugam, J. Guo, T. J. Boltje, V. V. Popik and G. J. Boons, *J. Am. Chem. Soc.*, 2011, **133**, 949–957.

12 P. A. Ledin, F. Friscourt, J. Guo and G. J. Boons, *Chem. – Eur. J.*, 2011, **17**, 839–846.

13 C. Ornelas, J. Broichhagen and M. Weck, *J. Am. Chem. Soc.*, 2010, **132**, 3923–3931.

14 J. A. Johnson, J. M. Baskin, C. R. Bertozzi, J. T. Koberstein and N. J. Turro, *Chem. Commun.*, 2008, 3064–3066.

15 S. V. Orski, A. A. Poloukhtine, S. Arumugam, L. D. Mao, V. V. Popik and J. Locklin, *J. Am. Chem. Soc.*, 2010, **132**, 11024–11026.

16 A. Kuzmin, A. Poloukhtine, M. A. Wolfert and V. V. Popik, *Bioconjugate Chem.*, 2010, **21**, 2076–2085.

17 A. Bernardin, A. Cazet, L. Guyon, P. Delannoy, F. Vinet, D. Bonnaffe and I. Texier, *Bioconjugate Chem.*, 2010, **21**, 583–588.

18 P. Gobbo, S. Novoa, M. C. Biesinger and M. S. Workentin, *Chem. Commun.*, 2013, **49**, 3982–3984.

19 M. Milne, P. Gobbo, N. McVicar, R. Bartha, M. S. Workentin and R. H. E. Hudson, *J. Mater. Chem. B*, 2013, **1**, 5628–5635.

20 Y. H. Kim, J. Jeon, S. H. Hong, W. K. Rhim, Y. S. Lee, H. Youn, J. K. Chung, M. C. Lee, D. S. Lee, K. W. Kang and J. M. Nam, *Small*, 2011, **7**, 2052–2060.

21 J. C. Olivier, R. Huertas, H. J. Lee, F. Calon and W. M. Pardridge, *J. Pharm. Res.*, 2002, **19**, 1137–1143.

22 F. Zhang, E. Lees, F. Amin, P. R. Gil, F. Yang, P. Mulvaney and W. J. Parak, *Small*, 2011, **7**, 3113–3127.

23 W. Fritzsche and T. A. Taton, *Nanotechnology*, 2003, **14**, R63–R73.

24 E. M. Sletten and C. R. Bertozzi, *Org. Lett.*, 2008, **10**, 3097–3099.

25 E. J. Kim, D. W. Kang, H. F. Leucke, M. R. Bond, S. Ghosh, D. C. Love, J. S. Ahn, D. O. Kang and J. A. Hanover, *Carbohydr. Res.*, 2013, **377**, 18–27.

26 M. Golkowski and T. Ziegler, *Synthesis*, 2013, **45**, 1207–1214.

27 R. van Geel, G. J. M. Pruijn, F. L. van Delft and W. C. Boelens, *Bioconjugate Chem.*, 2012, **23**, 392–398.

28 P. Gobbo and M. S. Workentin, *Langmuir*, 2012, **28**, 12357–12363.

29 M. C. Bourg, A. Badia and R. B. Lennox, *J. Phys. Chem. B*, 2000, **104**, 6562–6567.

30 D. G. Castner, K. Hinds and D. W. Grainger, *Langmuir*, 1996, **12**, 5083–5086.

31 R. C. Amos, A. Nazemi, C. V. Bonduelle and E. R. Gillies, *Soft Matter*, 2012, **8**, 5947–5958.

32 H. Ismaili, A. Alizadeh, K. E. Snell and M. S. Workentin, *Can. J. Chem.*, 2009, **87**, 1708–1715.

33 W. Limapichat and A. Basu, *J. Colloid Interface Sci.*, 2008, **318**, 140–144.

34 J. L. Brennan, N. S. Hatzakis, T. R. Tshikhudo, N. Dirvianskyte, V. Razumas, S. Patkar, J. Vind, A. Svendsen, R. J. M. Nolte, A. E. Rowan and M. Brust, *Bioconjugate Chem.*, 2006, **17**, 1373–1375.

35 M. X. Zhang, B. H. Huang, X. Y. Sun and D. W. Pang, *Langmuir*, 2010, **26**, 10171–10176.

36 W. J. Sommer and M. Weck, *Coord. Chem. Rev.*, 2007, **251**, 860–873.

37 L. F. Zhang and A. Eisenberg, *Science*, 1995, **268**, 1728–1731.

38 B. M. Discher, Y. Y. Won, D. S. Ege, J. C. M. Lee, F. S. Bates, D. E. Discher and D. A. Hammer, *Science*, 1999, **284**, 1143–1146.

39 H. Kim, Y. J. Kang, S. Kang and K. T. Kim, *J. Am. Chem. Soc.*, 2012, **134**, 4030–4033.

40 P. Tanner, P. Baumann, R. Enea, O. Onaca, C. Palivan and W. Meier, *Acc. Chem. Res.*, 2011, **44**, 1039–1049.

41 R. Chen, D. J. G. Pearce, S. Fortuna, D. L. Cheung and S. A. F. Bon, *J. Am. Chem. Soc.*, 2011, **133**, 2151–2153.

42 J. He, Z. J. Wei, L. Wang, Z. Tomova, T. Babu, C. Y. Wang, X. J. Han, J. T. Fourkas and Z. H. Nie, *Angew. Chem., Int. Ed.*, 2013, **52**, 2463–2468.

43 Y. Ofir, B. Samanta and V. M. Rotello, *Chem. Soc. Rev.*, 2008, **37**, 1814–1823.

This journal is © The Royal Society of Chemistry 2014

J. Mater. Chem. B, 2014, **2**, 1764–1769 | **1769**